Nonlinear Response of a Weakly Damaged Metal Sample: A Dissipative Modulation Mechanism of Vibro-Acoustic Interaction

V. ZAITSEV
Mechanical Engineering Department, Katholieke Universiteit Leuven, Celestijnenlaan 300 B, B-3001, Heverlee, Belgium, and Institute of Applied Physics RAS, 46 Uljanova Str., 603600, Russia

P. SAS
Mechanical Engineering Department, Katholieke Universiteit Leuven, Celestijnenlaan 300 B, B-3001, Heverlee, Belgium

(Received 24 March 1999; accepted 4 August 1999)

Abstract: The nonlinear vibro-acoustic response of solid samples containing quite a small amount of defects can be anomalously high in magnitude compared to the case of undamaged intact solids. Functional dependencies of the nonlinear effects exhibit rather interesting behavior. In this paper, experimental results on nonlinearity-induced cross-modulation of a high-frequency (HF) $f = 15 - 30$ kHz signal by a low-frequency (LF) $F = 20 - 60$ Hz vibration in an aluminum plate with a small single crack are reported. Comparison with a reference sample (the identical plate without a crack) has proven that the presence of such a small defect can be easily detected due to its nonlinear manifestations. It is demonstrated that under proper choice of the sounding signal parameters, the effect level can be so pronounced that the amplitude of the modulation side-lobes originated due to the nonlinearity exceeds the amplitude of the fundamental harmonic of the HF signal. Main functional features of the observed phenomena are analyzed, and a new physical explanation is suggested based on a dissipative mechanism of vibro-acoustic interaction. Results of the numerical simulation of the effect are also presented.

Key Words: Nonlinear response, nonlinear vibro-acoustics, diagnostics, cracks

1. INTRODUCTION

Nonlinear vibrational and acoustical effects in solids with microinhomogeneities have attracted ever-increasing attention during the past years in view of their possible applications in diagnostic problems (Antonets, Donskoy, and Sutin, 1986; Sutin, 1992; Rudenko, 1993; Korotkov and Sutin, 1994; Zaitsev et al., 1995; Zaitsev, 1998; Johnson, Sutin, and Van Den Abeele, 1999; Van Den Abeele et al., 1999). Conventionally in vibro-acoustic diagnostics, nonlinear distortions are intentionally eliminated or simply neglected and the information on the defects is extracted from the change of the linear response of the investigated sample (Collacott, 1985; Richardson and Mannan, 1992; Fritzen, Jennewein, and Kiefer, 1998). On the other hand, as experiments have proven, occurrence of quite a small amount of defects in a

Journal of Vibration and Control, 6: 803-822, 2000

solid may change its nonlinear parameters by orders of magnitude while the linear properties may be only slightly perturbed (Naugolnykh and Ostrovsky, 1998). Therefore, nonlinear distortions of a vibrational (acoustical) signal can be used as a very sensitive indicator of damage in the sample structure. Drastic differences in linear and nonlinear manifestations of microdefects in solids are now confirmed by numerous experimental demonstrations (Nazarov and Zimenkov, 1993; Johnson and Rasolofosaon, 1996), and general reasons of such difference are comprehended theoretically (see, for example, Zaitsev, 1996).

However, the nonlinear effects are too rich in variety to be explained in a unified way. It often happens that conventional quadratic or cubic nonlinearities of the material constitutive equation that are used in "classical" theory of nonlinear elasticity are insufficient to describe the observed phenomena (Naugolnykh and Ostrovsky, 1998). For example, experiments indicate that the microstructure-induced nonlinearity is in many cases not of purely elastic type, and sometimes it has a hysteretic or nonlinear-dissipative character (Nazarov et al., 1988; Nazarov, 1994; Johnson and Rasolofosaon, 1996). The procedure of identification of the type of nonlinearity is not evident. Apparently, the same nonlinear effects (e.g., generation of combination- or subharmonics) may be caused by nonlinearities of a different nature. To identify the particular nonlinear governing equation, it is necessary to study detailed functional properties of the nonlinear response (for example, its amplitude or frequency dependencies). Therefore, after first promising demonstrations (Antonets, Donskoy, and Sutin, 1986; Korotkov and Sutin, 1994) of the high "structural sensitivity" of nonlinear effects, further theoretical and experimental studies are required to reach a better understanding of the phenomena, which should provide more reliable extraction of information on the material structural changes from experimental data.

When setting up practical diagnostics, one should realize that the magnitude of the nonlinear components can remain small compared to the linear ones, although the level of nonlinear distortions in a damaged solid sample can be significantly increased due to the influence of the defects. Therefore, for practical applications, one should avoid masking nonlinear distortions both in electrical circuits and in vibro-acoustical actuators and sensors. It is also important to choose the most sensitive and, at the same time, robust nonlinear effects to observe. From that point of view, the use of the interaction (cross-modulation) of vibro-acoustical excitations with significantly different frequencies yields several advantages (Korotkov and Sutin, 1994). Such modulation effects are normally absent in weakly nonlinear undamaged (intact) homogeneous samples, and their noticeable level indicates the presence of some microstructure, for example, cracks in the investigated sample.

Since earlier observations of such nonlinear cross-modulation (Korotkov and Sutin, 1994), a whole series of experimental demonstrations of the effect was carried out in different conditions (Sutin et al., 1995; Nazarov and Zimenkov 1993; Ekimov, Didenkulov, and Kazakov, 1998; Johnson et al., 1999). In theory, the wave interaction in a damaged intact sample with a single discontinuity-like defect was analyzed by Zaitsev et al. (1995). The case of cross-modulation in a solid resonator made of a microinhomogeneous medium with multiple microdefects was considered by Nazarov and Zimenkov (1993). However, in many cases, those theoretical results are not sufficient to explain significant features of the experimental results (especially those obtained for single cracks that are small compared to the acoustic wavelength). Moreover, the simple intuitive deduction that a low-frequency action changes the propagation conditions through the crack for the acoustic wave is insufficient to explain satisfactorily the experimental results.

In the next section, experimental data are presented on the cross modulation of a high-frequency (HF) signal ($f = 15 - 30$ kHz) by a low-frequency (LF) vibration ($F = 10 - 60$ Hz) in an aluminum plate with a small single crack. Comparison with a reference sample (the identical plate without a crack) has proven that the influence of such a small defect on the nonlinearity of the sample can be easily detected. It is demonstrated that under proper choice of the sounding signal parameters, the effect may be significantly increased up to the extreme extent when the amplitude of the modulation side-lobes originated due to the nonlinearity exceeds the amplitude of the fundamental harmonic of the initial HF signal. Consequently, the discussion of main physical features of the observed effects is given. Using the revealed functional features of the phenomena and the performed estimates, a new physical explanation of the effects is suggested based on a dissipative mechanism that was not accounted for in the previous theoretical analysis. The simulation results obtained in the framework of the proposed mechanism are shown to be in agreement with the experimental data.

2. EXPERIMENT

2.1. Experimental Setup

The experimental setup is schematically shown in Figure 1(a). As seen in the figure, the sample (1), an aluminum plate (130 × 55 mm in sizes and 0.5 mm in thickness), was mounted on a shaker (2) through an intermediate piezo-actuator (3). The LF vibrations of the shaker and the HF oscillations of the piezo-actuator were controlled by independent signal generators (4), (5). Therefore, it was possible to excite simultaneously an LF vibration and an HF acoustic signal and to exclude the mixing of the signals in electrical circuits and in the actuators. The plate was tightly glued in its center to the piezo-actuator. Vibro-acoustic response of the plate was registered by lightweight accelerometers (6), (7), (8) located at the plate edges and in the center. After amplifier (9), the forms of the signals were monitored by a two-channel oscilloscope (10) and their spectrum was analyzed by a two-channel signal analyzer (11).

Two initially identical samples were used in the study. The plate without defects served as a reference sample. The second plate had a small transversal crack 5 mm in length located at 50 mm from one of the short plate edges (as shown in Figure 1(a)). The in-plane location of the crack in the plate is shown in Figure 1(b). The crack was previously produced due to vibrational fatigue at intensive vibrations of the plate clamped to the shaker.

The shaker excited the lowest bending mode of the plate. Resonant frequencies of HF vibrations were influenced by the exact position of the accelerometers and by the position of the connection with the exciter. However, for the effects described below, exact identification of the HF modes was not very important.

Note, finally, that the strain amplitude of the LF vibration was always higher (by the order of magnitude or more) than the strain amplitude of the HF vibration. Unlike the strain itself, the velocity of the strain change for the LF vibration could be already comparable or even significantly less than that of the HF oscillations due to the large difference in the high and low frequencies ($f/F \approx 500 - 800$).

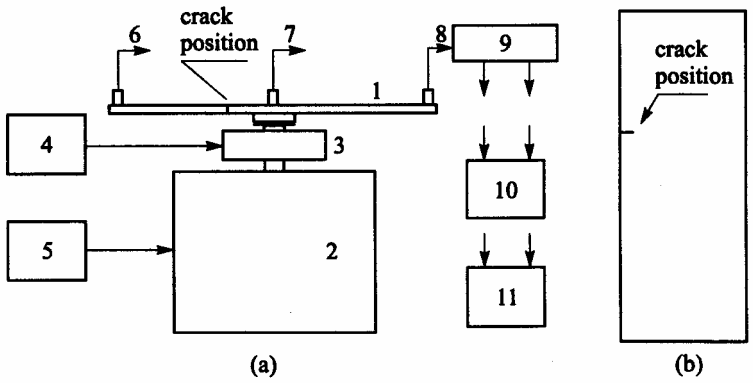

Figure 1. Schematically shown the experimental setup (a) and the in-plane location of the crack in the sample (b).

2.2. Results of the Observations

As it was mentioned in the introduction, the observation of the cross modulation of the HF signal under simultaneous excitation of the plate at low and high frequencies was used to detect nonlinearity of the samples. Both plates were exposed to the same excitation level in the same frequency band. The response of accelerometer 7 located at the connection region can be considered as an "input" signal and the signal of the side accelerometers corresponds to an "output." Such distinction is more valid for the LF vibration and is certainly only approximate to the HF case. In the response at LF, both plates behaved rather similarly: the lowest bending resonance of both plates was about 60 Hz. Both the LF and the HF resonance frequencies changed by a few percentage points when the positions of the accelerometers and of the connection region were changed by 1 to 2 centimeters. Thus, there was no definite distinction between the plates in their linear response. Quite different was the situation for their nonlinear response at the higher frequencies.

First, the HF response of the undamaged sample was studied. Under simultaneous excitation of both the LF and the HF vibrations, weak modulation side-lobes at $f \pm F$ were observed around the fundamental frequency f. The amplitude of the side-lobes increased proportionally to excitation amplitudes at both initial frequencies. The modulation was distinguishable at the side (see Figure 1(a)) accelerometers 6 and 8, and it was practically below the noise level for the central accelerometer 7. For different frequencies f within the band 15 to 40 kHz, the level of the modulation varied only slightly. However, even at a rather intensive LF vibration, the level of the side-lobes remained 60 to 40 dB lower than the central line f. A typical example of the spectrum at intensive excitation of the reference intact sample is shown in Figure 2. In the figure, the difference in the level of the side-lobes compared to the central line is about -51 dB.

For the damaged sample under analogous excitation conditions, the cross-modulation looked significantly different both quantitatively and qualitatively. First, the level of modulation was considerably higher (by 20 or even up to 50 dB). The corresponding example for exactly the same frequencies and the same LF acceleration as shown for the reference

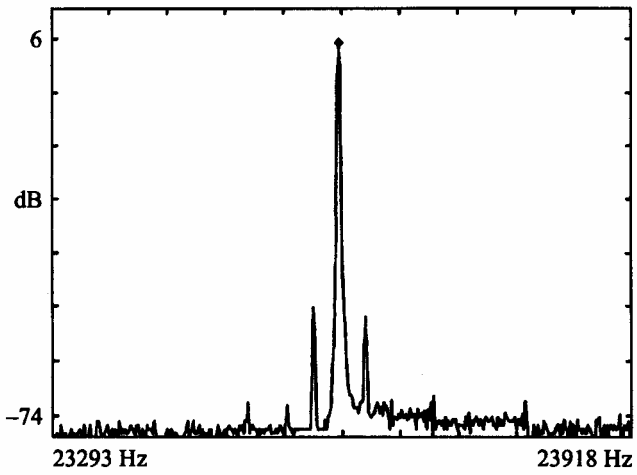

Figure 2. Modulation spectrum for the reference sample.

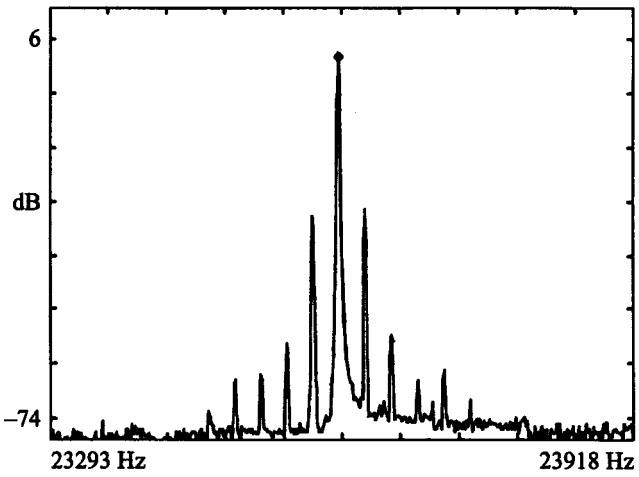

Figure 3. Modulation spectrum for the damaged sample at the same conditions as for Figure 2.

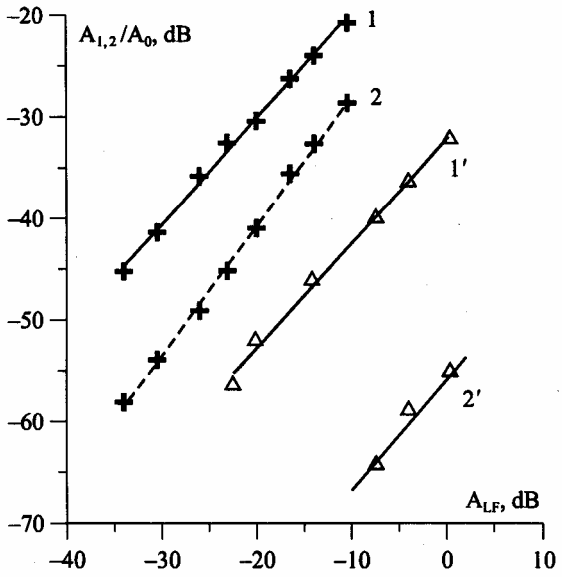

Figure 6. Relative level of the first (1 and 1′) and the second (2 and 2′) modulation side-lobes against the amplitudes of the LF vibration. Crosses, the damaged sample; triangles, the intact sample. The solid best-fit lines correspond to the linear dependency; the dashed line corresponds to the power law with exponent equal to 1.3.

sample in Figure 2 is presented in Figure 3 for the damaged plate. In this case, the relative level of the first-order side-lobes is already −27 dB (that is, 24 dB higher compared to −51 dB in Figure 2). Second, in most cases, the modulation spectrum contained significant amounts of higher side-lobes at frequencies $f \pm nF$, sometimes with numbers n up to 10 to 15. An example of such a rich spectrum is shown in Figure 4. The level of the LF vibration was even significantly lower compared to the case shown in Figure 3.

It is interesting that in this figure the level of the second- and third-order side-lobes is even higher compared to the first-order ones. The spectral features varied significantly with change of the high frequency, but the level of the side-lobes always was at least 10 to 15 times higher than in the reference sample. At some frequencies, the modulation was extremely strong, so that the central (fundamental) spectral line was several decibels lower than the side-lobes (see example in Figure 5).

Comparison of Figures 2 through 5 demonstrates that the nonlinear response of the damaged sample was drastically different from that of the undamaged reference plate. The modulation spectra essentially differed in their qualitative appearance, and quantitatively the level of the side-lobes in case of the damaged sample was increased by 10 to 15 times at least.

Figure 6 shows the quantitative difference between the damaged and the intact samples in the amplitudes of the first- and second-modulation side-lobes relative (in decibels) to the amplitude of the fundamental HF harmonic. The dependencies shown in this figure correspond to the spectral forms similar to those presented in Figures 2 and 3. The relative

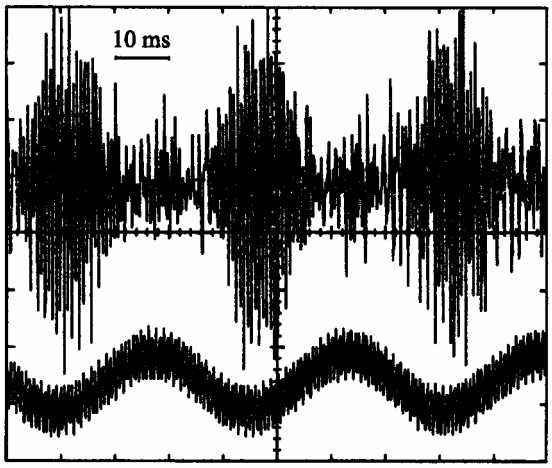

Figure 7. Temporal record of the vibration in the damaged sample at a strong modulation.

level of the modulation in the damaged sample is more than 20 dB higher for the first side-lobe, and more than 40 dB higher for the second side-lobe. The slope of the best-fit lines in the log-log plot in Figure 6 indicates that in both samples the amplitude of the first side-lobes depends approximately linearly on the LF vibration amplitude in the LF dynamic band presented in the figure. Further on at higher modulation level, the first-order side-lobes increased more slowly, but a rapid growth of higher order side-lobes was observed (we shall discuss those features in more detail in the next section). Figure 6 shows also that even at moderate modulation, the higher order side-lobes in the damaged sample increased more rapidly with the increase of the amplitude of the LF vibration (see the dashed best-fit line for the second-order side-lobes in Figure 6).

It is significant that at some frequencies f, the change in the amplitude was rather pronounced not only for the modulation side-lobes but also for the fundamental harmonic itself. Moreover, the effect looked apparently irregular since sometimes either increase or decrease in the amplitude of the fundamental harmonics was observed. We shall return to the explanation of such features in the discussion in the following section.

Finally, besides the time-averaged spectral parameters, the setup allowed for direct observation of the temporal dependence of the HF signal level at different phases of the LF vibration. An example of such a time record made by a two-channel digital oscilloscope is shown in Figure 7. This example corresponds to the higher amplitude of the LF vibrations. The lower record displays the input signal of accelerometer 7 where both the LF and the HF signals are present. The upper record shows the output of accelerometer 8, but the LF signal component is filtered out by a high-pass filter. There is a strong modulation of the HF output signal. In the spectral representation, such a modulation corresponded to the occurrence of strong multiple side-lobes ($f \pm nF, n = 1, 2, 3, \ldots$) as shown in Figures 4 and 5.

Summarizing the experimental data, it may be concluded that introduction of a weak damage (a small fatigue crack) caused a drastic increase in nonlinear vibro-acoustic response of the damaged sample. Those nonlinear modulation effects allow for easy distinction

between the damaged and the intact reference sample. In the next section, we shall discuss the main features of the observed phenomena in more detail.

3. DISCUSSION

3.1. Does Elastic Nonlinearity Suffice to Explain the Observed Modulation?

The answer to this question is not evident as, in principle, pure elastic nonlinearity of contacts between the crack edges may cause both phase and amplitude modulation of a wave transmitting through the crack. Such a problem was analyzed, for example, in Zaitsev et al. (1995). It was mentioned that for small deformation of a crack under the influence of the LF vibration, one can use the Tailor expansion of the effective relation between the stress applied to the crack and its strain. Then, the main (first) nonlinear term in the "stress-strain" relation should be quadratic in the deformation. However, this term is not sufficient to explain the occurrence of numerous intensive side-lobes $f \pm nF$ in the modulation spectrum due to the interaction of the initially excited harmonics with frequencies F and f. In case of the quadratic nonlinearity, only the first side-lobes should be observed in the modulation spectrum. One may argue that those components could be attributed to the existence of initial LF spectral components nF ($n = 2, 3 \ldots$), which are transformed to higher frequencies $f \pm nF$ due to the quadratic nonlinearity. Indeed, due to the own nonlinearity of the shaker, several higher components occurred in the initial spectrum of the LF excitation, but their initial level was too small to explain the existence of very high side-lobes like those shown in Figures 3 and, especially, 4 and 5. The same discrepancy was observed in the experiments (Ekimov, Didenkulov, and Kazakov, 1998) on vibro-acoustic cross modulation due to a cracklike defect for torsional HF and longitudinal LF waves in a rod sample.

One may also assume that in case of significant closing and opening of the crack under the LF action, it is more reasonable to approximate the effective stress-strain relation for the crack by some almost piecewise function (like a piecewise-linear characteristic of a diode in electronics). In principle, for such a type of the nonlinearity, numerous spectral side-lobes could be produced when an HF wave is propagating through the crack that is "breathing" in a piecewise manner under the action of purely sinusoidal LF excitation. However, in the discussed experiment, the interaction process cannot be treated as the quasi-one-dimensional propagation of the HF wave through the breathing crack, like it was considered in Zaitsev et al. (1995). Namely, in the discussed experiment, the crack was too small and could not be considered as an effective screen even for the HF waves. Its sizes both in thickness and in length were much smaller than the HF wavelength and the transversal size of the plate.

To estimate the influence of a crack in such a case, one can use another approach. Let us take into account that the amplitude of strain in LF excitation is strong compared to the strain in the HF signal. Therefore, we can consider the breathing of the crack as a given motion under the action of the LF excitation. Thus, to estimate maximal influence on the HF signal, it is enough to compare the extreme cases when the crack is totally closed and totally opened under the LF action.

Then, one could take into account that the size of the plate in its axial direction was several times greater than that in the transversal direction. Therefore, the plate could be considered as a quasi-one-dimensional structure along its axis. Thus, we may describe the plate as a rod or a beam with a small crack in one of its cross sections. When the crack is closed, the structure

is uniform along its axis, so that effective modulus E of the axial stiffness of the plate-beam $E(x) = E_0 = const.$ When the crack is opened because of the applied LF flexural action, the effective modulus becomes inhomogeneous along the axis: $E(x) = E_0 + \delta E(x)$. The localized decrease $\delta E(x)$ of the plate stiffness can be approximated by a Π shape form:

$$\delta E(x) = \begin{cases} -\Delta E, & \text{at } x \in [x_0, x_0 + l] \\ 0, & \text{at } x \notin [x_0, x_0 + l] \end{cases}, \tag{1}$$

where x_0 is the crack position and l corresponds to its thickness. The value of the decrease ΔE is easily related to the defect geometry. As the crack cuts the whole thickness of the plate, the maximal value of the stiffness decrease ΔE is determined by the crack length h in the transversal direction to the plate axis:

$$\Delta E/E_0 \approx h/H, \tag{2}$$

where H is the plate width.

Now it is possible to estimate the influence of the crack on the natural frequencies of the plate. For example, we can consider the case of lowest HF modes of longitudinal waves, which should have practically uniform structure along the plate width for the used frequencies $f = 15 - 30$ kHz. Then, the wave equation for the longitudinal stress σ along the plate axis takes the form

$$\sigma_{tt} - \frac{E(x)}{\rho}\sigma_{xx} = 0. \tag{3}$$

Equation (3), together with boundary conditions at the plate ends $x = 0$ and $x = L$, determines the mode structures $\varphi_n(x)$ along the plate axis and the modal natural frequencies ω_n. Neglecting the masses of the accelerometers, we can write that

$$\sigma(0) = \sigma(L) = 0. \tag{4}$$

For boundary conditions (4) and the uniform stiffness $E(x) = E_0$, equation (3) yields the following for the unperturbed modal functions:

$$\varphi_n(x) = \sin(\pi nx/L). \tag{5}$$

Assuming the harmonical dependence of stress $\sigma \propto \exp(i\omega t)$ and using the conventional procedure of the perturbation theory, one could obtain the expression for the relative change of the normal mode frequencies:

$$\frac{\delta\omega_n}{\omega_n} = \frac{1}{2}\frac{\int_0^L \frac{\delta E(x)}{E_0}\varphi_n^2(x)dx}{\int_0^L \varphi_n^2(x)dx}. \tag{6}$$

Therefore, in the discussed case, equations (1), (5), and (6) yield for the perturbations of the modal frequencies

$$\delta\omega_n/\omega_n \approx \sin^2\left(\frac{\pi n x_0}{L}\right)\frac{l}{L}\frac{\Delta E}{E_0}. \tag{7}$$

It is evident from (7) that the exact knowledge of the boundary conditions and the corresponding exact modal forms are not significant for the estimate of the maximal effect of the crack. Indeed, for quantitative estimation of the maximal possible influence of the crack, it is enough to take into account that $\sin^2(\pi n x_0/L) \leq 1$. It should be also taken into account that the crack thickness l in the experiment was not larger than 0.1 mm. Thus, for the plate axial length $L \approx 130$ mm, we obtain that the relation $l/L \leq 7.7 \cdot 10^{-4}$. Furthermore, taking into account the crack length $h \leq 5$ mm and the plate width $H \approx 50$ mm, equation (1) yields that the relation $\Delta E/E_0 \approx h/H \leq 10^{-1}$. Substitution of those estimates in equation (7) gives for the shift of the resonant frequency:

$$|\delta\omega_n/\omega_n| = |\delta f_n/f_n| \leq 7.7 \cdot 10^{-5}, \tag{8}$$

where $f_n = \omega_n/(2\pi)$. The real value of the perturbation should be even significantly smaller, as estimate (8) corresponds to the difference between the extreme cases when the crack is fully opened or fully closed. In the given test conditions, the crack cannot be opened or closed totally by the LF vibrations. But even the highest estimate (8) for the used frequencies at 15 to 30 kHz corresponds to the maximal possible shift δf_n of the normal mode frequencies f_n by about 0.5 to 1 Hz. Typical width Δf_n of the resonance peaks in the experiment was about 150 to 200 Hz (which corresponded to the quality factor $Q = f_n/\Delta f_n = 100 - 150$). Therefore, to explain the observed strong modulation effects by a shift of the resonance frequency, the resonance shift δf_n should be comparable with the width Δf_n of the resonance peaks. That is, there should be $\delta f_n \approx 10 - 100$ Hz, which is almost 2 orders of magnitude higher than the maximal estimate (8).

The above estimate was derived for the case of the wave equation (3) for a longitudinal wave; however, those results are not limited to the longitudinal waves. Indeed, for the bending waves in a thin plate, the displacement ς obeys the fourth-order wave equation instead of the second-order equation (3) (Landau and Lifshitz, 1986):

$$\zeta_{tt} - \frac{D(x)}{\rho d}\zeta_{xxxx} = 0, \tag{9}$$

where $D = Ed^3/12(1-\nu^2)$, d is the plate thickness, ν is the Poisson ratio for the plate material, and ρ is its density. Evidently, the relative disturbance of the bending stiffness $\delta D(x)/D$ is the same as $\delta E(x)/E$. Although the natural frequencies themselves are different for the longitudinal and the bending waves, equation (9) yields the same results (6) and (7) for the relative perturbation of the natural frequencies as it was obtained from equation (3). Consequently, the quantitative estimate (8) remains the same for the bending waves. Thus, the conclusion that the observed modulation cannot be attributed to the perturbation of the plate natural frequencies remains valid for the bending modes also.

Table 1.

U_{HF} (V)	2	5	6	10
$A_0/\tilde{A}_0$	1.34	1.35	1.35	1.37

3.2. Main Features of the Dependence of the HF Signal Losses on the LF Action

The above-mentioned qualitative features of the modulation and the quantitative discrepancies between the estimates and the measurements lead to the conclusion that the observed effects could not be caused by the influence of the LF vibration via purely elastic nonlinearity of the system. Therefore, we should admit that the observed modulation was caused by some nonlinear mechanism of the influence of the LF vibration on the losses of the high-frequency wave. To describe and simulate the physical origin of the phenomena, it is necessary to reveal the main functional dependencies of the observed effects.

Let us discuss the main time-averaged functional dependencies of the LF-induced losses that were experimentally elicited. First, the HF excitation was tuned to an HF resonance of the sample (for example, $f = 20085$ Hz), and the amplitudes of the fundamental HF harmonic were compared when the LF action was switched on or turned off. The level of the LF vibration was fixed, while several different amplitudes of the HF excitation were used in the measurements. It was revealed that due to the LF influence, the amplitude of the HF fundamental harmonic decreased by the same factor for different levels of the HF excitation. This statement is illustrated by Table 1, in which U_{HF} is the voltage of the HF generator and $A_0/\tilde{A}_0$ is the relation of the amplitudes of the HF fundamental harmonic when the LF vibration was switched off and turned on, correspondingly.

Then, it was noticed that the amplitudes of the side-lobes $f \pm nF$ were linearly proportional to the amplitude of the fundamental HF harmonic at given LF amplitude. This statement is illustrated by Figure 8, where the amplitudes of the fundamental and the lowest four modulation harmonics are plotted against the voltage amplitude U_{HF} of the HF generator. The results presented in Figure 8 were obtained for a resonance peak $f = 26210$ Hz at moderate amplitude of the LF vibration (that is, the spectrum form was similar to those shown in Figure 3). Other resonance peaks demonstrated similar dependencies. These results indicated that the HF losses remained linear in the amplitude of the HF excitation, although they were dependent on the LF vibration amplitude.

In such a case, for the HF signal, the total decrement θ (that is conventionally defined as a value inversely proportional to the quality factor $Q = \pi/\theta$) can be written in the following form:

$$\theta = \theta_l + \theta_n . \tag{10}$$

Here, θ_l corresponds to linear losses when the amplitude of the LF action tends to zero and $\theta_n = \theta_n(A_{LF})$ corresponds to the change of the decrement due to the influence of the LF vibrations. To estimate the dependence $\theta_n(A_{LF})$, another series of measurements of the HF harmonics amplitude was carried out at given HF excitation levels and different LF vibration amplitudes (the same HF resonance was used). The results are graphically shown in Figure 9. It is essential to note that at lower amplitudes of the LF vibration (below -25 dB in the scale of Figure 9), the absolute value of the decrease of the fundamental harmonic amplitude was

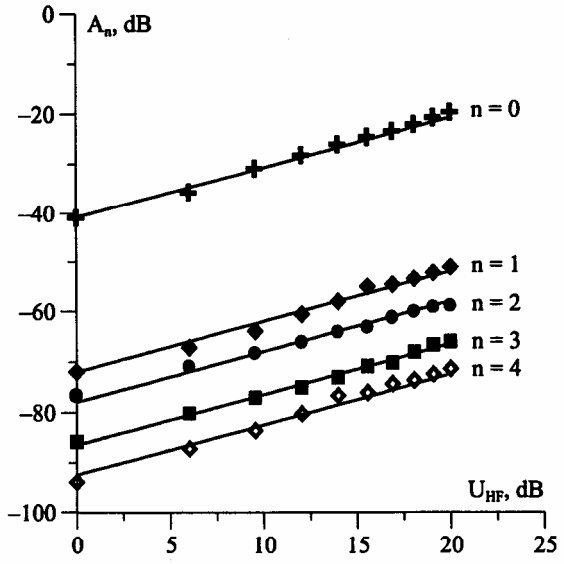

Figure 8. Dependencies of the fundamental HF harmonic ($n = 0$) and the modulation side-lobes ($n = 1 - 4$) on the amplitude of the HF excitation. The solid lines correspond to the linear law.

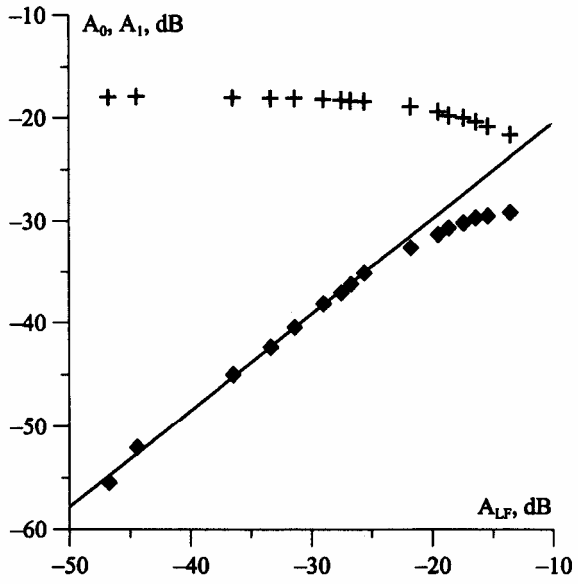

Figure 9. Dependencies of the fundamental harmonic (crosses) and the first modulation side-lobe (diamonds) on the amplitude of the LF vibration. The solid line corresponds to the linear dependence.

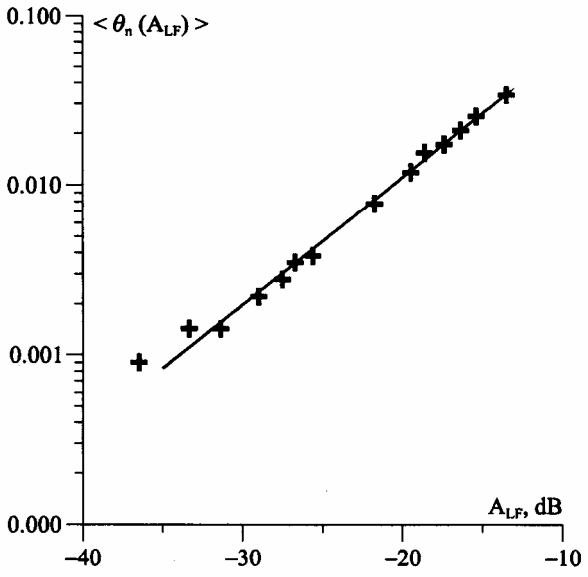

Figure 10. Period-averaged $< \theta_n(A_{LF}) >$ as a function of amplitude A_{LF} (recalculated from the data presented in Figure 9). The solid line corresponds to the power law with exponent 1.5.

significantly (several times) less than the amplitude of the modulation side-lobe. The latter depended almost linearly on the LF vibration amplitude at the lower excitation (the solid line in Figure 9 corresponds to such a linear dependence). With further increase of the LF vibration amplitude, the first-order side-lobe got to saturation, whereas pronounced multiple higher-order side-lobes appeared in the spectrum. The decrease of the fundamental HF harmonic became also more pronounced at higher amplitudes, as it is shown in Figure 9.

Attributing the decrease of the fundamental harmonic to the additional losses $\theta_n(A_{LF})$ (according to equation (10)), the decrease of the fundamental harmonic can be recalculated to the dependence $< \theta_n(A_{LF}) >$. Here the angle brackets denote the averaging over the period of the LF vibration. Thus, we may estimate the averaged additional losses as

$$< \theta_n(A_{LF}) >= \frac{2\pi}{Q_0}\left(\frac{A_0(A_{LF})}{A_0(0)} - 1\right), \tag{11}$$

where Q_0 is the initial quality-factor of the resonance peak at $A_{LF} = 0$. It was determined that for the resonance $f = 20085$ Hz to which the data plotted in Figure 9 correspond, the HF resonance peak width at -3 dB level was $\Delta f \approx 200$ Hz. The corresponding quality factor $Q_0 = f/\Delta f \approx 100$. Using this estimate together with the data plotted in Figure 9 and expression (11), the averaged value $< \theta_n(A_{LF}) >$ was calculated. The obtained dependence is presented in Figure 10. It appeared to be close to a power law $\theta_n \propto A_{LF}^q$ with exponent $q \approx 1.5$, which was determined by the slope of a best-fit line in the log-log plot. Analogous measurements were carried out for other HF resonance peaks, which gave similar results (both qualitatively and quantitatively) to that described above.

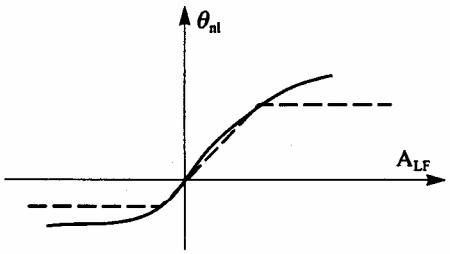

Figure 11. Qualitative behavior of the nonlinear losses (the solid curve) and their approximation by a piecewise function (the dashed curve).

Note that the obtained period-averaged function $< \theta_n (A_{LF}) >$ may be significantly different compared to the instantaneous dependence $\theta_n (A_{LF})$. To reconstruct the latter, it is necessary to take into account the direct temporal observation of the amplitude modulation of the HF signal in addition to the spectral (time-averaged) measurements. Example of such a temporal record is presented, for example, in Figure 7. The figure shows that there is significant difference in the amplitude of the HF signal between different half-periods of the LF action. The latter fact indicates that the transversal structure of the crack was essentially asymmetrical. Indeed, in case of a symmetrical structure of the crack, there should not be such a difference between bending of the plate at positive and negative angles. If the crack were symmetrical, only even modulation harmonics ($f \pm 2F, f \pm 4F, \ldots$) should be observed. In reality, at low excitation, mainly the first modulation harmonics $f \pm F$ were noticeable instead of $f \pm 2F$.

To explain the observed variety of spectral and temporal properties, one should admit that at lower amplitudes, the nonlinear additive θ_n is almost a linear antisymmetrical function of the LF deformation $\theta_n (A_{LF}) \propto A_{LF}$. This approximation looks rather natural as the first term of the expansion of $\theta_n (A_{LF})$ into the Tailor series at $A_{LF} \rightarrow 0$. Indeed, for such a law, there should not be change in the amplitude of the fundamental harmonic at lower amplitude A_{LF}, as function $\theta_n (A_{LF})$ is almost odd and the period-averaged additional losses are absent. However, instantaneous change of the decrement $\theta_n (A_{LF})$ is proportional to the instantaneous value $A_{LF}(t)$, which should produce the first-order modulation side-lobes in the spectrum. Then, one should admit that at higher amplitudes A_{LF}, function $\theta_n (A_{LF})$ should demonstrate noticeable asymmetry and tendency to saturation. The latter properties are essential to explain the asymmetry in the modulation (see the temporal record in Figure 7) as well as the saturation in absorption and the rapid growth of higher-modulation harmonics with the increase of the LF vibration amplitude. In Figure 11, the solid line shows qualitatively the above-mentioned features of the nonlinear variation of the HF losses $\theta_n (A_{LF})$. Certainly, one may choose various analytical approximations for such a function to fit the observation results. For example, for numerical simulation, it is convenient to approximate such a dependence by a piecewise-linear function (the dashed line in Figure 11).

3.3. Hysteretical or Purely Dissipative Nonlinearity?

The analysis of the experimental data in the previous section allowed for the phenomenological reconstruction of the functional form of the nonlinearity-induced losses. However, such a reconstruction yet does not give an idea on the physical nature of the effect, and it is interesting to discuss this question too. For example, the best known type of material nonlinearity that influences both the elastic properties and the absorption of vibrations is the hysteretic nonlinearity. It is well-known (Naugolnykh and Ostrovsky, 1998) that in case of hysteretical nonlinearity, the losses due to hysteresis are dependent on the excitation amplitude. However, in our experiment, the losses of the HF vibration depended only on the LF vibration amplitude but behaved as conventional viscouslike linear losses with respect to the amplitude of the HF oscillations. Further on, if the losses were caused by a hysteretical nonlinearity, they should be accompanied by a noticeable change in elastic (reactive) properties of the system, that is, there should be the shift of resonant frequencies. However, in the experiment, the significant change in the signal amplitude was not accompanied by a comparable change in the resonance frequencies. Therefore, we cannot accept the assumption that the nonlinear mechanism has the hysteresis character. It is necessary to admit that the LF action significantly influenced just the dissipative properties of the system without significant effect on its elastic properties.

Alternatively, the observed viscouslike HF losses may be attributed to the thermal dissipation of the acoustical energy at the contacts of the crack edges. Despite the small volume of the crack, those losses are significantly increased due to high-temperature gradients at the vicinity of the crack edges. Those gradients are not determined by the acoustic wavelength, but by the scale of the interedge microcontacts that is significantly less. A similar thermal mechanism is responsible for the anomalously strong sound dissipation in polycrystalline media (see Landau and Lifshitz, 1986). This effect alone might give the increase of the thermal losses by 2 to 3 orders of magnitude and more (depending on the vibration frequency). In our case, however, there is an additional important strong factor: the increased amplitude of the deformation of the microcontacts inside the crack, as they are much softer (also probably by 2-4 orders) compared to the stiffness of the surrounding intact material. Those combined factors could cause the thermal losses at a rather small crack, which are comparable to other losses in the whole sample. In principle, such a strong dissipation in a cracked material is a well-known effect, for example, for a cracked glass. In the discussed experiment, the applied LF action changed the amount and the stiffness of the contacts at the crack, causing the modulation of the viscouslike thermal losses of the HF waves.

3.4. Resonance Effects

Resonant effects are also essential for the comprehension of the experimental results. As the modulation frequency (in most cases, about 15-30 Hz) was an order of magnitude smaller than the width of the resonance peaks, it is possible to consider the influence of the LF vibration as a quasi-static action. Then, in the maximum of a resonance peak, it is possible to estimate the HF sample response $A_{HF}(t)$ (and then to obtain the modulation spectrum) by simple multiplication of the HF sinusoidal input signal and the quality-factor $Q(t) = 2\pi/(\theta_l + \theta_n)$, which is influenced by the LF vibration though decrement $\theta_n = \theta_n(A_{LF}(t))$:

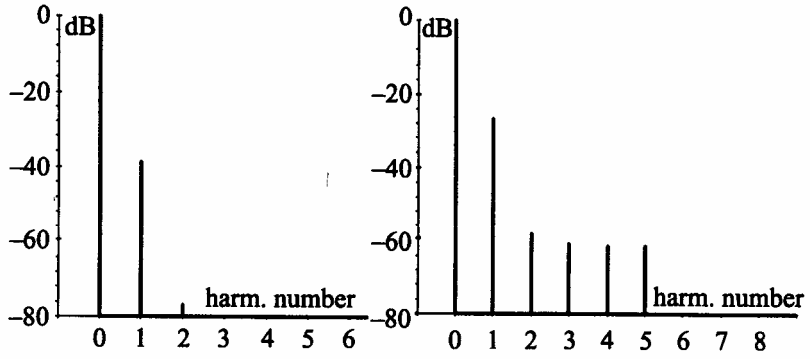

Figure 12. Example of the simulation of the modulation spectra at lower (left) and higher (right) LF vibration amplitudes.

$$A_{HF}(t) \propto \sin(2\pi f \cdot t) \cdot Q(t) = \frac{\pi \cdot \sin(2\pi f \cdot t)}{\theta_l + \theta_n \left(A_{LF}^0 \sin(2\pi F \cdot t)\right)}, \tag{12}$$

where $A_{LF}(t) = A_{LF}^0 \cdot \sin(2\pi \mathrm{F} \cdot \mathrm{t})$. For the numerical simulation, it is convenient to use the piecewise-linear approximation of $\theta_n(A_{LF})$ as it is shown in Figure 11. Examples of the calculations are presented in Figure 12. In the figure, for the lower LF vibration amplitude that falls within the initial linear part of the dependence $\theta_n(A_{LF})$, only the first side-lobes are noticeably present (left part of the figure). At a higher level when the saturation of the function $\theta_n(A_{LF})$ is important already, multiple $f \pm nF$ side-lobes pronouncedly appear in the modulation spectrum (right part of the figure).

In addition to the resonance case, another convenient possibility to observe the modulation is the use of narrow antiresonances. In case of a deep enough antiresonance, the central line at the fundamental frequency can be suppressed while the modulation side-lobes could become even higher, as it was shown in Figure 5, which was obtained just at one of the sample antiresonances. Unlike a resonance, in an antiresonance, additional losses may cause not the decrease, but the increase of the amplitude of the fundamental HF harmonic.

The above-mentioned features of the antiresonance case gave a possibility to verify the conclusion on the decisive role of the dissipation factor by carrying out the following instructive experiment. First, the HF excitation was tuned to an antiresonance of the damaged plate, and a strong modulation spectrum was obtained (see Figure 13(a)). Then several light and soft porous rubber strips were stuck to the plate surface to introduce additional HF losses with minimal perturbation of the sample mass and stiffness. The strips caused the decrease of the sample Q-factor by more than 2 times, which was checked later on by measuring the widths of a few resonance peaks. As for the modulation, the relative level of the modulation side-lobes decreased by about 20 dB (see Figure 13(b)), which should not happen if the nonlinear elasticity were responsible for the modulation. Besides the decrease of the side-lobes, Figure 13 shows that the introduction of the strong additional losses caused the increase of the amplitude of the fundamental harmonic by 5 dB, which was also expected for the

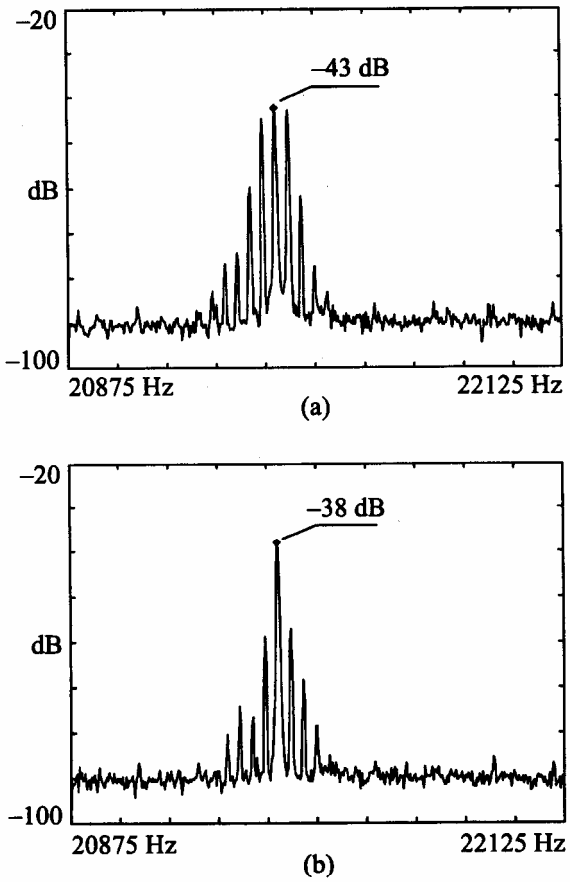

Figure 13. The modulation spectrum for the damaged sample before (a) and after (b) the introduction of additional losses by sticking the rubber strips.

antiresonance case. Thus, the observed variety of the measured functional dependencies and other features of the modulation is self-consistently explained by the suggested dissipative mechanism.

4. CONCLUSIONS

Experimental results presented in the paper are an interesting example of a rather strong nonlinear vibro-acoustic manifestation of a weak damage in a solid. The obtained data show that the modulation nonlinear effects could be effectively used for detection of even small cracklike defects in a metal sample. The performed estimates proved that the influence of the crack on the change of the sample linear stiffness (and, therefore, on conventionally measured resonance frequencies) was negligibly small and could be hardly detected by conventional linear methods.

The observed variety of features of the nonlinear vibro-acoustic interaction is self-consistently explained by the influence of the LF vibration on the thermal viscouslike losses of the weak HF oscillations due to deformation of the contacting crack edges. Certainly the suggested dissipative mechanism is not the unique one, and, at different conditions, other mechanisms (elastic or hysteretic nonlinearities) may be also important. In particular, the vibro-acoustic interaction due to the elastic nonlinearity of a crack (Zaitsev et al., 1995) should be important when the crack square is comparable to the cross section of the whole sample. However, the results obtained in the present work indicate that for small cracks that cannot perturb significantly the sample stiffness, the proposed dissipative mechanism of the nonlinear interaction plays the main role. Therefore, the use of nonlinear effects associated with the modulation of the dissipation might be a very effective tool for crack diagnostics. The revealed features of the mechanism allow for better choosing of the parameters of the vibro-acoustic action to provide the best conditions for defect diagnostics.

Note, finally, that the described study was aimed primarily at revealing the mechanism of the nonlinear response of a small crack, while the important question about the damage location was omitted. In principle, a combination of a time-gating procedure (which is conventional for linear acoustic nondestructive testing) with the observation of nonlinearity-induced signal components can be suggested to provide spatial resolution in nonlinear diagnostics. Such a principle was discussed, for example, in Zaitsev et al. (1995). However, simple time-gating can eliminate resonance effects, the use of which is very advantageous for high sensitivity of crack detection. Alternatively, to provide spatial resolution by means of local excitation of a defect, resonance vibration modes with different shapes can be used. Therefore, it is difficult to suggest a universal solution, and particular cases of sample geometry and defect type require special consideration.

Acknowledgments. The authors are grateful to Dr. A. Osipov for useful discussions of the measurement technique. The work was supported by a grant of the Research Council of the Katholieke Universiteit Leuven.

REFERENCES

Antonets, V. A., Donskoy, D. M., and Sutin, A. M., 1986, "Nonlinear vibrodiagnostics of delayer in layer construction," *Mechanics of Composite Materials* **5**, 934-937 (in Russian).

Collacott, R. A., 1985, *Structural Integrity Monitoring*, Chapman & Hall, London, UK.

Ekimov, A. E., Didenkulov, I. N., and Kazakov, V. V., 1998, "Nonlinear acoustic phenomena in a rod with a crack," in *Proceedings of the 3rd International Conference of Acoustical and Vibratory Surveillance*, Senlis, France, pp. 481-489.

Fritzen, C. P., Jennewein, D., and Kiefer, T., 1998, "Damage detection based on model updating methods," *Mechanical Systems and Signal Processing* **12**(1), 163-186.

Johnson, P. A. and Rasolofosaon, P.N. J., 1996, "Manifestation of nonlinear elasticity in rock: Convincing evidence over large frequency and strain intervals from laboratory studies," *Nonlinear Processes in Geophysics* **3**, 77-88.

Johnson, P. A., Sutin, A., and Van Den Abeele, K. E-A., 1999, "Application of nonlinear wave modulation spectroscopy to discern material damage," in *Proceedings of the 2nd International Conference, Emerging Technologies in NDT*, Athens, Greece, May.

Korotkov, A. S. and Sutin, A. M., 1994, "Modulation of ultrasound by vibrations in metal constructions with cracks," *Acoustics Letters* **18**, 59-62.

Landau, L. D. and Lifshitz, E. M., 1986, *Theory of Elasticity*, Pergamon, Elmsford, NY.

Naugolnykh, K. and Ostrovsky, L., 1998, *Nonlinear Wave Processes in Acoustics*, Cambridge University Press, Cambridge, UK.

Nazarov, V. E., 1994, "Self-action of elastic waves in media with dissipative nonlinearity," *Acoustics Letters* **17**(8), 145-149.

Nazarov, V. E., Ostrovsky, L. A., Soustova, I. A., and Sutin, A. M., 1988, "Nonlinear acoustics of micro-inhomogeneous media," *Physics of the Earth and Planetary Interiors* **50**(1), 65-73.

Nazarov, V. E. and Zimenkov, S. V., 1993, "Sound by sound modulation in metallic resonators," *Acoustics Letters* **16**(9), 198-201.

Richardson, M. and Mannan, M. A., 1992, "Remote detection and location of structural faults using modal parameters," in *Proceedings of 10th International Conference on Modal Analysis (IMAC)*, San Diego, CA, September, pp. 502-507.

Rudenko, O. V., 1993, "Nonlinear methods of acoustical diagnostics," *Defectoscopia* **8**, 24-32 (in Russian).

Sutin, A. M., 1992, "Nonlinear acoustic diagnostics of micro-inhomogeneous media," in *Proceedings of the International Symposium on Recent Advances in Surveillance Using Acoustical and Vibrational Methods*, Senlis, France, pp. 497-506.

Sutin, A. M., Korotkov, A. S., Didenkulov, I. N., Kim, E. J., and Yoon, S. W., 1995, "Nonlinear acoustic methods for crack and fatigue detection," in *Proceedings of Physical Acoustic Workshop, Safety Diagnostics of Underwater Constructions by Using Acoustics*, Kaist, Seoul Branch, Seoul, Korea, pp. 43-55.

Van Den Abeele, K. E. A., Carmeliet, J., TenCate, J. A., and Johnson, P. A., 1999, "Single mode nonlinear resonant acoustic spectroscopy (SIMONRAS) for damage detection in quasi-brittle materials," in *Proceedings of the 2nd International Conference, Emerging Technologies in NDT*, Athens, Greece, May.

Zaitsev, V. Yu., 1996, "A model of anomalous acoustic nonlinearity of microinhomogeneous media," *Acoustics Letters* **19**(9), 171-176.

Zaitsev, V. Yu., 1998, "Nonlinear acoustic manifestations as an informative sign of structural changes in non-destructive interrogation problems," in *Proceedings of the 3rd International Conference Acoustical and Vibratory Surveillance*, Senlis, France, pp. 409-418.

Zaitsev, V. Yu., Sutin A. M., Belyaeva I. Yu., and Nazarov V. E., 1995, "Nonlinear interaction of acoustical waves due to cracks and its possible usage for cracks detection," *Journal of Vibration and Control* **1**(3), 335-344.